RSC Advances

RSC Advances

www.rsc.org/advances

ROYAL SOCIETY
OF CHEMISTRY

www.rsc.org/advances

ARTICLE TYPE

Mixed-Morphology and Mixed-Orientation Block Copolymer Bilayers

Nicolás A. García[a], Raleigh L. Davis[b], So Youn Kim[b,c], Paul M. Chaikin[d], Richard A. Register[b], and Daniel A. Vega*[a]

Block copolymers have attracted considerable attention due to their ability to self-assemble into highly regular structures, spanning length scales from several nanometers to over 100 nm. Block copolymers confined in thin films have been extensively utilized as soft templates for nanofabrication, but most
10 applications have been restricted to single-layer templates with smectic and hexagonal symmetries. Here we show that a multi-step approach that includes shear alignment, thin film lift-off, and stacking can access novel three-dimensional block copolymer structures with long-range order and mixed symmetries. This technique allows control over the long-range order and also expands the range of nanolithographic templates accessible through guided self-assembly.

15

Introduction

Over the past two decades, there has been a growing demand for cost-effective nanofabrication technologies for different applications, ranging from electronics or optoelectronics to
20 nanofluidics, photovoltaics, and molecular filters, among others. Among self-assembling systems, block copolymers[1,2] have emerged as attractive templates due to their capacity to generate ordered structures at the nanoscale, high resolution, cost-effectiveness, and compatibility with traditional processing
25 techniques.[3-5] By controlling the molecular structure of a block copolymer, it is possible to obtain a wide variety of nanostructures with prescribed chemical, mechanical, electronic, or transport properties. In bulk, block copolymers have been employed to fabricate, for example, nanoporous materials[6] and
30 drug delivery systems,[7] and as templates to arrange nanoparticles via selective sequestration.[4,5] In thin films, block copolymers have already demonstrated their usefulness as templates for the fabrication of nanowire polarizing grids,[8] ultra-high-density arrays of nanowires[9] and nanodots,[10,11] and high-density magnetic
35 media.[12]

The equilibrium structures of block copolymers are determined by molecular topology, block sequence, composition, molecular size, and the interaction parameters among the chemically distinct block units. In block copolymers with relatively simple
40 architectures, such as AB diblocks and ABA triblocks, the structures include phases with spherical, cylindrical, double gyroid, or lamellar nanodomains.[1,2] However, upon increasing the complexity of the molecular architecture the number of accessible equilibrium structures can become enormous.[13] Also, upon

45 confinement in nanodroplets or nanofibers the equilibrium morphologies observed in the bulk can be frustrated and therefore new structures and symmetries emerge.[14-16] Confinement into thin films also can frustrate the symmetry observed in the bulk, and depending on the confining length scales, and the affinity of each
50 block for the interfaces, a wide variety of morphologies can be obtained.[3,4,17,18]

As one of the main drawbacks of the self-assembly strategy is the lack of long-range order due to the presence of defects, a significant effort has been devoted to producing well-ordered
55 patterns. A variety of techniques, including graphoepitaxy, shear flow, electric fields, or a sweeping temperature gradient, have been employed.[3,5,19-24] These nanodomain patterns can then be used as templates for devices that require well-ordered structures, such as magnetic recording media or flash memories.
60 Most approaches that depend on self-assembled patterns have focused on controlling a block copolymer film containing only a single layer of nanodomains, such as spheres or cylinders lying parallel or standing perpendicular to the substrate.[4,5] However, recently there has been a growing interest in obtaining more
65 complex three-dimensional (3D) structures.[17,25,26] The self-assembly of block copolymers in 3D presents similar drawbacks as in 2D: spontaneous self-organization always leaves defects[27-29] that for most applications should be avoided. In addition, even with templating to eliminate the defects, the achievable
70 symmetries are limited. For example, the confining surfaces usually have a preferential affinity for one block in the copolymer, so in lamellae-forming thin films the domains tend to lie parallel to the substrate for film thicknesses which are an integer multiple of the interdomain spacing; islands or holes form
75 if the average film thickness is incommensurate with this

characteristic spacing.[5] In bilayers of block copolymers with spherical[30] or cylindrical[31,32] structure, the nanodomain lattices in each layer share a common orientation but are laterally shifted with respect to each other. In recent work, Jeong et al. used shear alignment of a polystyrene-poly(dimethylsiloxane) diblock copolymer to fabricate a bilayer of oriented silicon oxide (SiOx) lines, in which the orientation angle between layers could be independently controlled; in this case, the first layer of block copolymer was reduced to SiOx lines by plasma etching prior to the deposition of the second layer, so that only one layer of block copolymer was present at any point in the process flow.[33]

Here we present an experimental method to produce out-of-equilibrium structures via the stacking of thin films of block copolymers with smectic and hexagonal symmetries. This method imparts independent control over the long-range order and orientation of shear-aligned cylinders in each layer of a bilayer film, and also allows combining block copolymers with different domain symmetries or chemical compositions.
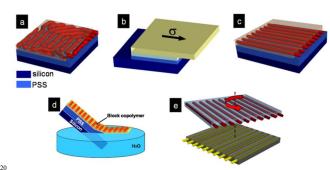

Figure 1. Schematic process flow of the bilayer preparation method. Panel a: the block copolymer is spin coated onto a sacrificial layer of PSS spun directly onto a silicon wafer. Panels b and c: shear alignment is employed to obtain patterns with long-range orientational order. Panel d: once aligned, the block copolymer is floated off onto a water surface. Panel e: as the shear direction, and therefore the cylinders' dominant orientation, is known, the floated film can be redeposited onto a pattern with a different orientation.

Materials and Methods

Figure 1 shows the schematic process flow employed to obtain the ordered block copolymer thin film bilayers. This multistep process involves spin coating, shear alignment, thin film liftoff in water, and film redeposition onto a well-ordered block copolymer monolayer. Since the stacking process occurs at room temperature, well below the glass transition temperature of the minority block in the copolymer, the individual layers retain the symmetry and structure established during the shear alignment. As this technique requires floating the polymer on a water surface, we employed a sacrificial layer of a water-soluble polymer:[34] poly(4-styrenesulfonic acid), PSS (Sigma-Aldrich), with a weight-average molecular weight of 75 kg/mol. The PSS was obtained as an 18 wt.% aqueous solution; the solution was evaporated to near dryness and the polymer redissolved in 2-propanol (Fisher, ACS grade) to form a 1 wt.% solution, from which a 40-50 nm layer of PSS was spin-coated onto a silicon wafer. Silicon wafers, purchased from Silicon Quest International, were prewashed with toluene and dried under

flowing nitrogen before polymer deposition. After drying of the PSS layer at room temperature, a 37 nm layer of a poly(styrene)-poly(n-hexylmethacrylate), PS-PHMA, diblock copolymer (PS-PHMA 33/78) was spin-coated onto the PSS-coated wafer from a 1 wt. % solution in toluene, a good solvent for both blocks but a nonsolvent for PSS. The film thickness was measured using ellipsometry (Gaertner Scientific LS116S300, λ= 632.8 nm).

The PS-PHMA diblocks employed here were synthesized via sequential living anionic polymerization of styrene and n-hexyl methacrylate, in tetrahydrofuran at -78°C, using 10 eq of LiCl to s-butyllithium initiator.[35,36] The cylinder-forming diblock (PS-PHMA 33/78) had number-average block molar masses of 33 and 78 kg/mol for PS and PHMA, respectively, and diblock dispersity Đ = 1.06, while the sphere-forming diblock (PS-PHMA 18/95) had block molar masses of 18 and 95 kg/mol and Đ = 1.08.

In addition to the two PS-PHMA diblocks, a cylinder-forming polystyrene-poly(ethylene-alt-propylene) diblock copolymer, PS-PEP 4/13, was also examined. This block copolymer, with number-average block molar masses of 4.3 and 13.2 kg/mol for PS and PEP, was synthesized through sequential living anionic polymerization of styrene and isoprene, followed by selective saturation of the isoprene block.[37]
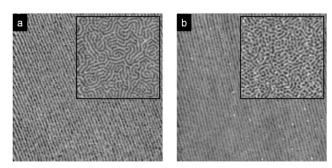

Figure 2. AFM phase images (size = 2 μm × 2 μm) of shear-aligned cylinder-forming PS-PHMA 33/78 deposited at monolayer thickness onto a bare silicon wafer (panel a) and a PSS-coated wafer (panel b). The insets show AFM phase images corresponding to both films in the unaligned state (inset image size = 1 μm × 1 μm).

While thermal treatments above the glass transition temperatures of both blocks can be employed to improve the degree of order in the block copolymer pattern, this process is prohibitively slow for most technological purposes.[28,29] In addition, as there are no preferential directions that break the azimuthal symmetry, thermal annealing does not allow control over the macroscopic orientation of the cylinders. To obtain well-ordered structures oriented in a prescribed direction, the PS-PHMA 33/78 films were shear-aligned on a hot plate at 150 °C, above the glass transition temperatures of both blocks, using 10 kPa of pressure and 5 kPa of shear stress, applied through a 1 × 1 cm^2 cross-linked polydimethylsiloxane pad for 30 min.[21] The films were then cooled below the glass transition temperature of the PS block to lock in the structure induced by shear, prior to removing the stress. A similar process was employed to shear align a monolayer of cylinder-forming PS-PEP 4/13, at 130°C.

AFM images were acquired using a Veeco Dimension 3000 in tapping mode with uncoated Si tips having a cantilever length of 125 μm, spring constant of 40 N/m, and resonant frequency of

~300 kHz. Phase and height AFM images were flattened to improve image quality. Scanning electron microscopy (SEM) images were obtained with a FEI Quanta 200 environmental scanning electron microscope under high vacuum.

5

Results and Discussion

Figure 2 shows tapping-mode atomic force microscopy (AFM) phase images of a PS-PHMA 33/78 monolayer spun onto a bare 10 silicon wafer (panel a) or a PSS-coated wafer (panel b). The repeat spacing for PS-PHMA 33/78 is 39 nm (as measured on thin films by AFM) and the cylinders adopt a configuration parallel to the substrate because of interfacial energy differences between the chemically dissimilar blocks. As the spin-coating 15 solvent evaporates, the order-disorder temperature of the thin film increases above room temperature and the blocks form a nanodomain structure that unavoidably contains a high density of defects, since the nanodomain grains nucleate randomly and with uncorrelated orientations, as shown in the insets of Fig. 2. The 20 main panels in Fig. 2 show the pattern configurations after shear alignment; these micrographs are characteristic of the degree of alignment over the whole sheared area. Note in both images the absence of disclinations and that the pattern exhibits long-range orientational order; the only defects are isolated dislocations 25 (with an areal density of order 1 per μm^2). The quality of shear alignment is excellent on both the bare[21] and PSS-coated wafers.
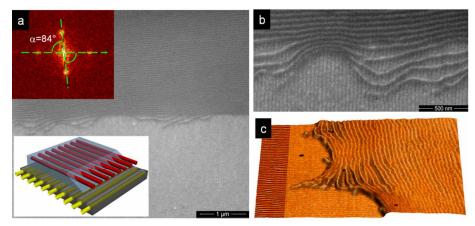

Figure 3. SEM images (panels a and b) of a stacked bilayer of PS-PHMA 33/78, both taken near the edge of the top layer, at different magnifications. The 30 top inset in panel (a) shows the power spectrum S(q) of the SEM data, revealing that the rotation angle α between the cylinders in the two layers is 84°. This power spectrum was obtained through two-dimensional fast Fourier transformation. Panel c shows a height-phase AFM image of the same system. In the darker leftmost region of panel (c), the AFM image of the lower layer has been filtered in Fourier space to emphasize the orientation of the cylinders (AFM image size = 1 μm × 1.36 μm).

Once the sample was aligned, the silicon-PSS-(PS-PHMA) 35 multilayer was introduced into a Petri dish containing deionized water, at an angle of about 45° to the water surface, to float off the block copolymer thin film (Fig. 1d). The floating thin film was immediately picked up from below the water surface, using a second silicon wafer onto which a monolayer PS-PHMA film had 40 been spun-coated and shear-aligned under identical conditions.

As the orientation of the cylinders in both systems is known from their respective shear directions, it is possible to overlap the layers at any prescribed angle (Fig. 1e). Figure 3 shows a scanning electron microscopy (SEM) image of a block copolymer 45 bilayer. The precise value of the rotation angle α = 84° can be obtained from the Fourier transform shown in the top inset of Fig. 3a.
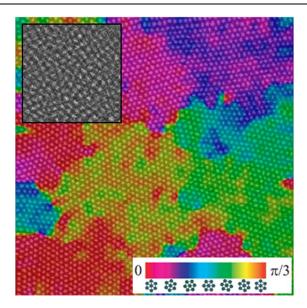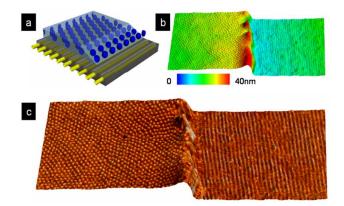
Figure 4. AFM phase image of a thermally annealed monolayer of sphere-forming PS-PHMA 18/95, with the local bond orientation θ indicated according to the color map shown at lower right. Image size: 2.0 μm × 2.0 μm. Inset: the as-spun block copolymer thin film presents only short-range order.

This method also allows combining block copolymers with different compositions or nanodomain symmetries. Here the stacking procedure was also employed to obtain bilayers of cylinder-forming polymers with different chemical structures, and to stack sphere-forming and cylinder-forming block copolymers. To obtain stacks combining cylinder- and sphere-forming PS-PHMA diblocks, a monolayer (35 nm) of sphere-forming PS-PHMA 18/95 was spun onto a sacrificial layer of PSS. Since the as-spun film presents a structure with a high defect density and only short-range order (see the inset of Figure 4), the PSS-(PS-PHMA) system was thermally annealed under vacuum at 125 ºC for 16 hours. Figure 4 shows an AFM phase image of the annealed PS-PHMA 18/95 film. By locating the spheres and applying a Delaunay triangulation, it is possible to determine the inter-sphere bond orientation θ, with regard to a reference axis[29] (see the colour map for the bond orientation θ in Figure 4) and then to evaluate the local orientational order parameter at a position r: $\psi(r) = \exp[6i\theta(r)]$. The azimuthally-averaged correlation function $g_6(r) = \langle \psi(r)\psi(0) \rangle$ was then calculated and the correlation length ξ_6 was measured by fitting $g_6(r)$ with $\exp[-r/\xi_6]$.[29] After thermal annealing, the correlation length of the PS-PHMA 18/95 film increases from ξ_6 ~30 nm to ~250 nm.

Figure 5 shows an AFM image of the sphere-forming PS-PHMA 18/95 film deposited on a shear-aligned cylinder-forming PS-PHMA 33/78 film. The hexagonal lattice constant for the sphere-forming top layer is 35 nm (as measured by AFM), and the step height of ~35 nm measured in the AFM image shown in Figure 5b is consistent with the film thickness measured through ellipsometry prior to water liftoff. Note that the upper surface of the PS-PHMA 18/95 top layer remains flat and that the degree of order in the hexagonal structure is unperturbed by the liftoff and redeposition.

Figure 5. Bilayer mixed-morphology film, unaligned spheres on top of shear-aligned cylinders, shown schematically in panel (a). Height-height (panel (b)) and height-phase (panel (c)) AFM micrographs. Image size: 1.4 μm × 0.6 μm.

In addition, the stacking method allows for the formation of multilayers from block copolymers with different chemical structures, as illustrated in Figure 6 for two shear-aligned cylinder-formers: PS-PEP 4/13 and PS-PHMA 33/78. In this case, the bottom layer is constituted by a 30 nm thick film of PS-PEP deposited onto on a bare silicon wafer while the second layer was made from PS-PHMA 33/78, redeposited following the procedure described above. Figure 6a shows an SEM image of the shear-aligned PS-PHMA 33/78 film prior to liftoff (PS-PEP cannot be imaged by SEM due to poor contrast), while Figures 6b and 6c show AFM phase images for the stacked bilayer, again taken near the edge of the top layer. Given the strong difference in viscoelastic behavior between the PHMA and PEP matrices in the two layers, a single set of AFM tapping mode conditions cannot simultaneously resolve the cylinders in both layers; therefore, the AFM images of Figures 6b and 6c were obtained using different values for the drive amplitude. Note that these two polymers also present a large difference in intercylinder spacings a: for PS-PEP 4/13, a=21 nm, while for PS-PHMA 33/78, a=39 nm.

RSC Advances

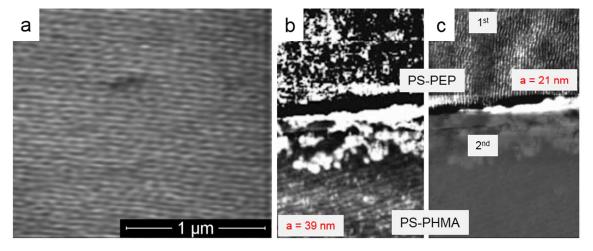Dynamic Article Links ▶

ARTICLE TYPE

Figure 6. Bilayer formed from shear-aligned block copolymers with different chemical structure. (a) SEM image of shear-aligned PS-PHMA 33/78 block copolymer monolayer film prior to liftoff. (b,c) AFM phase images of the stacked bilayer, taken near the edge of the top layer (PS-PHMA 33/78) to emphasize the differences in cylinder orientations in the layers formed from the different copolymers. AFM image size: 1.5 μm (height) × 1.0 μm
5 (width). AFM imaging conditions were chosen to emphasize either the PS-PHMA 33/78 top layer (panel (b)), or the PS-PEP 4/13 bottom layer (panel (c)).

Conclusions

In summary, this sequential layer stacking process allows the creation of 3D structures which would never form by
10 spontaneous self-assembly alone, such as cylinders stacked orthogonally (or at any angle), as well as mixed-morphology stacks. This process can facilitate the fabrication of ultradense arrays of phase-separated nano-domains with complex symmetries over large areas (~1 cm^2) and it is a potential
15 complement to conventional lithography to overcome the resolution limit of lithographic techniques. Note also that the application of this method is not restricted to the production of self-assembled templates or scaffolds for the production of nanostructured materials. For example, this approach could be
20 used to develop free-standing membranes with accurate control over the in-plane elastic anisotropy, ranging from pure liquid-crystalline to crystalline order.

Acknowledgments

Notes and references

^{a}Instituto de Física del Sur (IFISUR), Consejo Nacional de Investigaciones Científicas y Técnicas (CONICET), Departamento de Física. Universidad Nacional del Sur. Av. LN Alem 1253, 8000 Bahía
35 Blanca, Argentina. E-mail: dvega@criba.edu.ar
^{b}Department of Chemical and Biological Engineering, Princeton University, Princeton, NJ 08544, USA.
^{c}School of Energy and Chemical Engineering, Ulsan National Institute of Science and Technology, South Korea.
40 ^{d}Center for Soft Condensed Matter Research and Department of Physics, New York University, New York, NY 10003, USA.

DOI: 10.1039/b000000x/

45 1 F. S. Bates and G. H. Fredrickson, *Annu. Rev. Phys. Chem.*, 2003, **41**, 525–557.
2 M. W. Matsen and F. S. Bates, *Macromolecules*, 1996, **29**, 1091–1098.
3 A. P. Marencic and R. A. Register, *Annu. Rev. Chem. Biomol. Eng.*,
50 2010, **1**, 277–297.
4 S. B. Darling, *Prog. Polym. Sci.*, 2007, **32**, 1152–1204.
5 I. W. Hamley, *Nanotechnology*, 2003, **14**, R39–R54.
6 H. Mao and M. A. Hillmyer, *Soft Matter*, 2006, **2**, 57–59.
7 F. Meng, Z. Zhong and J. Feijen, *Biomacromolecules*, 2009, **10**, 197-
55 209.
8 V. Pelletier, K. Asakawa, M. Wu, D. H. Adamson, R. A. Register and P. M. Chaikin, *Appl. Phys. Lett.*, 2006, **88**, 211114.
9 T. Thurn-Albrecht, J. Schotter, G. A. Kästle, N. Emley, T. Shibauchi, L. Krusin-Elbaum, K. Guarini, C. T. Black, M. T. Tuominen and T.
60 P. Russell, *Science*, 2000, **290**, 2126–2129.
10 M. Park, P. M. Chaikin, R. A. Register and D. H. Adamson, *Appl. Phys. Lett.*, 2001, **79**, 257-259.
11 K. Shin, K. A. Leach, J. T. Goldbach, D. H. Kim, J. Y. Jho, M. Tuominen, C. J. Hawker and T. P. Russell, *Nano Lett.*, 2002, **2**, 933–
65 936.
12 K. Naito, H. Hieda, M. Sakurai, Y. Kamata and K. Asakawa, *IEEE Trans. Mag.*,2002, **38**, 1949–1951.

RSC Advances Accepted Manuscript

13   F. S. Bates, M. A. Hillmyer, T. P. Lodge, C. M. Bates, K. T. Delaney and G. H. Fredrickson, *Science*, 2012, **336**, 434-440.

14   Y. Wu, G. Cheng, K. Katsov, S. W. Sides, J. Wang, J. Tang, G. H. Fredrickson, M. Moskovits and G. D. Stucky, *Nature Materials*, 2004, **3**, 816-822.

15   M. Ma, K. Titievsky, E. L. Thomas and G. C. Rutledge, *Nano Letters*, 2009, **9**, 1678-1683.

16   P. Chen, H. Liang and A. C. Shi, *Macromolecules*, 2008, **41**, 8938-8943.

17   A. K. G. Tavakkoli, K. W. Gotrik, A. F. Hannon, A. Alexander-Katz, C. A. Ross and K. K. Berggren, *Science*, 2012, **336**, 1294-1298.

18   J. Chai and J. M. Buriak, *ACS Nano*, 2008, **2**, 489–501.

19   D. Sundrani and S. J. Sibener, *Macromolecules*, 2002, **35**, 8531–8539.

20   R. A. Segalman, A. Hexemer and E. J. Kramer, *Macromolecules*, 2003, **36**, 6831–6839.

21   D. E. Angelescu, J. H. Waller, D. H. Adamson, P. Deshpande, S. Y. Chou, R. A. Register and P. M. Chaikin, *Adv. Mater.*, 2004, **16**, 1736–1740.

22   D. E. Angelescu, J. H. Waller, D. H. Adamson, R. A. Register and P. M. Chaikin, *Adv. Mater.*, 2007, **19**, 2687–2690.

23   R. Ruiz, H. Kang, F. A. Detcheverry, E. Dobisz, D. S. Kercher, T. R. Albrecht, J. J. De Pablo and P. F. Nealey, *Science*, 2008, **321**, 936-939.

24   S. Park, D. H. Lee, J. Xu, B. Kim, S. W. Hong, U. Jeong, T. Xu and T. P. Russell, *Science*, 2009, **323**,1030-1033.

25   F. Rose, J. K. Bosworth, E. A. Dobisz and R. Ruiz, *Nanotechnology*, 2011, **22**, 035603.

26   B. K. Kuila, P. Formanek and M. Stamm, *Nanoscale*, 2013, **5**, 10849-10852.

27   C. Harrison, D. H. Adamson, Z. Cheng, J. M. Sebastian, S. Sethuraman, D. A. Huse, R. A. Register and P. M. Chaikin, *Science*, 2000, **290**, 1558–1560.

28   C. Harrison, Z. Cheng, S. Sethuraman, D. A. Huse, P. M. Chaikin, D. A. Vega, J. M. Sebastian, R. A. Register and D. H. Adamson, *Phys. Rev. E*, 2002, **66**, 011706.

29   C. Harrison, D. E. Angelescu, M. Trawick, Z. Cheng, D. A. Huse, P. M. Chaikin, D. A. Vega, J. M. Sebastian, R. A. Register and D. H. Adamson, *Europhys. Lett.*, 2004, **67**, 800–806.

30   G. E. Stein, E. J. Kramer, X. Li and J. Wang, *Macromolecules*, 2007, **40**, 2453–2460.

31   C. Harrison, M. Park, P. M. Chaikin, R. A. Register, D. H. Adamson and N. Yao, *Macromolecules*, 1998, **31**, 2185-2189.

32   R. Magerle, *Phys. Rev. Lett.*, 2000, **85**, 2749-2752.

33   J. W. Jeong, Y. H. Hur, H.-j. Kim, J. M. Kim, W. I. Park, M. J. Kim, B. J. Kim, and Y. S. Jung, *ACS Nano*, 2013, **7**, 6747-6757.

34   J. M. Torres, C. Wang, E. B. Coughlin, J. P. Bishop, R. A. Register, R. A. Riggleman, C. M. Stafford and B. D. Vogt, *Macromolecules*, 2011, **44**, 9040-9045.

35   S. K. Varshney, J. P. Hautekeer, R. Fayt, R. Jérôme and P. Teyssié, *Macromolecules*, 1990, **23**, 2618-2662.

36   H.-K. Kwon, V. E. Lopez, R. L. Davis, S. Y. Kim, A. B. Burns and R. A. Register *Polymer*, 2014, **55**, 2059-2067.

37   A. P. Marencic, D. H. Adamson, P. M. Chaikin and R. A. Register, *Phys. Rev. E*, 2010, **81**, 011503.

RSC Advances Accepted Manuscript

Graphical Abstract

5 Mixed-Morphology and Mixed-Orientation Block Copolymer
Bilayers by García et al.

10

Three-dimensional block copolymer structures with long-range
order and mixed symmetries.

15